A Neural Model of Dominating Opponent Inhibition in Visual On and Off Pathways for Robust Contour Extraction

Thorsten Hansen* and Heiko Neumann*

Universität Ulm, Abt. Neuroinformatik, D-89069 Ulm, Germany
Email: (hansen, hneumann)@neuro.informatik.uni-ulm.de

Abstract. In the primary visual pathway, information is represented in two distinct, complementary domains, namely on- and off-cells. In this work we examine how on- and off-cells may interact to form the input to simple cell subfields. We propose a mechanism of dominating opponent inhibition, where a simple cell subfield is driven by both domains, receiving stronger weighted input from the opponent pathway. We conduct a series of simulations employing synthetic test data as well as natural stimuli which show that the proposed circuit is robust to noise, largely independent of the amount of noise added. This unique property may give a rationale for the representation of contrast information in two complementary domains. Finally, we demonstrate that the model can account for physiological data on luminance gradient reversal recorded from simple cells in feline striate cortex. Based on these findings we hypothesize that the visual system realizes a mechanism similar to dominating opponent inhibition in order to robustly extract features in noisy environments.

1 Introduction

Processing of visual stimuli begins in the retina, where electromagnetic radiation within a certain frequency band is transformed into a neural code. One first major processing stage are retinal ganglion cells with center-surround receptive fields (RFs). Axons of ganglion cells form the optic nerve, which terminates in a relay structure of the thalamus, the lateral geniculate nucleus (LGN). LGN cells project upon the primary visual area V1 in the occipital lobe. Here, simple cells are found with a different RF structure than ganglion cells. Simple cells have elongated RFs and respond to bars of a certain orientation and position.

Several schemes have been proposed for the neural wiring of LGN cell afferents to subfields of simple cells. In the classical proposal of Hubel and Wiesel (1962), excitatory signals from on-cells drive the on-subfield, whereas excitatory signals from off-cells drive the off-subfield (Fig. 1, left). Another approach assumes that simple cells are driven by one type of ganglion cells alone (Heggelund, 1986). In this case, on-cell signals excite the on-subfield and inhibit the off-subfield (Fig. 1, middle).

* Supported by DFG (SFB 527).

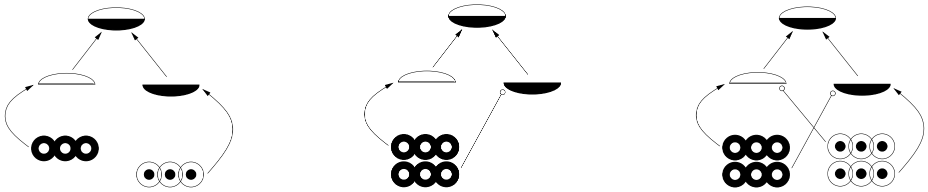

Fig. 1. Alternative combination schemes for LGN cells to drive simple cell subfields. Arrows denote excitatory input, circles at the end of lines inhibitory input. See text for details.

An alternative scheme of opponent inhibition has been proposed by Ferster (1989), in which the on-subfield receives excitatory input from the on-path and inhibitory input from the off-path. The reverse holds true for the off-subfield (see Fig. 1, right). This scheme is employed in a computational model of brightness perception (Pessoa, Mingolla, & Neumann, 1995; Neumann, Pessoa, & Hansen, 1999). Here, we extend this scheme and introduce an imbalance of excitatory/inhibitory inputs, namely a stronger weighting of inhibitory inputs in either subfield. With this mechanism of dominating opponent inhibition (DOI), the model is i) more robust to noise, ii) capable of reproducing physiological data of simple cell responses to luminance gradient reversal.

2 The Model

In this next section we give a short formal description of the model. Further details can be found in Neumann et al. (1999). The model consists of a hierarchical organization of two main processing stages, namely on- and off-cells, followed by a simple cell circuit. In all equations, Greek letters denote positive valued model parameters.

On- and off-cell responses are modeled via shunting interaction of isotropic center-surround RFs. For the on-cell, the equation reads

$$\widetilde{X}_{\mathrm{on}} = \frac{\beta_X I_{\mathrm{c}} - \gamma_X I_{\mathrm{s}}}{\alpha_X + I_{\mathrm{c}} + I_{\mathrm{s}}} \ , \tag{1}$$

where $I_{\mathrm{c}}, I_{\mathrm{s}}$ are input responses from center and surround RFs, resp., which are modeled by convolution of the input stimulus I with isotropic Gaussians of different standard deviations. Off-cell responses $\widetilde{X}_{\mathrm{off}}$ are modeled by interchanging I_{c} and I_{s}. Contrast responses are generated by cross-channel inhibition, which reads for the on-contrast

$$X_{\mathrm{on}} = \left[\widetilde{X}_{\mathrm{on}} - \widetilde{X}_{\mathrm{off}}\right]^{+} \ . \tag{2}$$

The off channel response is computed analogously. $[x]^{+} = \max\{x, 0\}$ denotes half-wave rectification.

Input to the simple cell subfields is sampled using elongated, oriented weighting functions G_θ with a smoothly decaying effective coupling strength. In order to have plateau-like RF profiles, properly aligned isotropic Gaussians with a distance of their standard deviation are summed to build the weighting function for the simple cell subfield. Before integration, contrast activity of different polarity competes at each spatial location. The new proposed scheme of dominating opponent inhibition introduces a positive constant $\xi > 1$ which scales the opponent contribution. Input activation for, e.g., the on-subfield is computed by

$$R_{\text{on},\theta} = \left[(X_{\text{on}} - \xi X_{\text{off}}) * G_\theta\right]^+ \ , \tag{3}$$

where $*$ denotes spatial convolution. The off-subfield activation $R_{\text{off},\theta}$ is generated accordingly. On- and off-subfields interact via a disinhibition circuit which boosts activities for spatially juxtaposed on- and off-contrast configurations. Simple cells are modeled for eight discrete orientations and for two opposite contrast polarities, namely light-dark and dark-light. The resulting simple cell activity consists of a linear and a nonlinear, i.e. multiplicative, term (Neumann et al., 1999)

$$\widetilde{S}_{\text{ld},\theta} = \frac{\alpha_S(R_{\text{on},\theta} + R_{\text{off},\theta}) + 2\beta_S(R_{\text{on},\theta} R_{\text{off},\theta})}{\alpha_S\gamma_S + \delta_S(R_{\text{on},\theta} + R_{\text{off},\theta})} \ . \tag{4}$$

Simple cells sensitive to opposite contrast polarity undergo mutual inhibition which sharpens the activity profile:

$$S_{\text{ld},\theta} = \left[\widetilde{S}_{\text{ld},\theta} - \widetilde{S}_{\text{dl},\theta}\right]^+ \ . \tag{5}$$

3 Responses in the Presence of Noise

In order to test the noisy response properties, we measured mean subfield responses (3) to a homogeneous region corrupted by additive Gaussian noise for different values of the weighting parameter ξ and different standard deviations of the Gaussian noise.

The results are depicted in Fig. 2. The abscissa denotes ξ, the ordinate denotes mean response. The curves correspond to Gaussian noise of standard deviation 0.32, 0.1, 0.032 (top to bottom), added to a homogeneous region. We observe that the mean response decreases as ξ gets larger and is almost zero for $\xi = 2$. Most interesting, this is true for all three curves, irrespectively of the amount of noise added. This adaptive behavior can be explained by (3), showing that with the noise getting larger, the inhibition from the opponent channel gets larger, too.

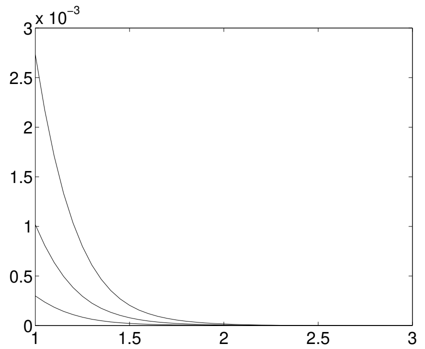

Fig. 2. Mean subfield responses to homogeneous regions for different amount of noise and varying $\xi \in [1; 3]$.

4 Simulations of 2D Stimuli

In this section we demonstrate the capacity of the model when probed with artificial as well as natural 2D stimuli. Model parameters are the same in all simulations. For the initial center-surround filtering, standard deviations of the Gaussians are set to $\sigma = 1$ for the center and $\sigma = 3$ for the surround. For the simple cells subfields, five isotropic Gaussians of standard deviation $\sigma = 2$ are summed, which results in an RF of about twice the size of the RF of the on- and off-cells. In the simulations, we compare the new mechanism of DOI (setting $\xi = 2$) to a linear simple cell model and to the nonlinear model without DOI ($\xi = 1$). For the linear model, subfield responses are added: $\widetilde{S}_{\mathrm{ld},\theta} = R_{\mathrm{on},\theta} + R_{\mathrm{off},\theta}$ (cf. (4)). The linear model approximates filtering with a first order Gaussian derivative (Neumann et al., 1999). The edge images shown are obtained by pooling simple cell responses of both contrast polarities for all orientations.

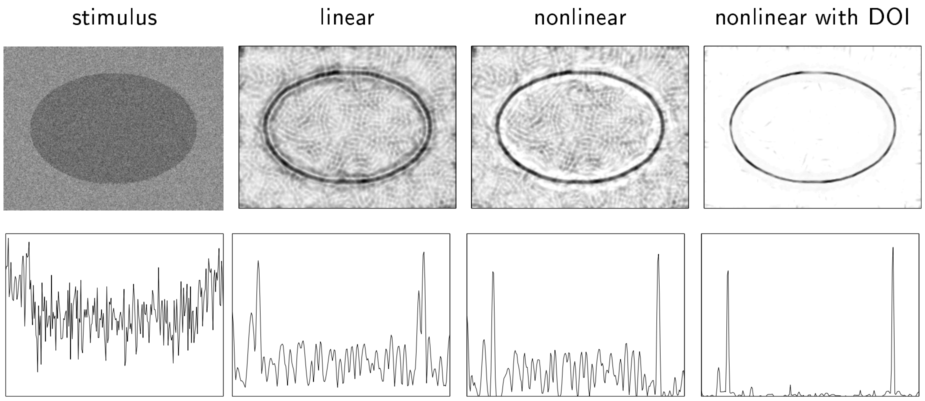

Fig. 3. Noisy input stimulus and simulation results (top row) together with the corresponding horizontal cross sections taken at the center of the images (bottom row).

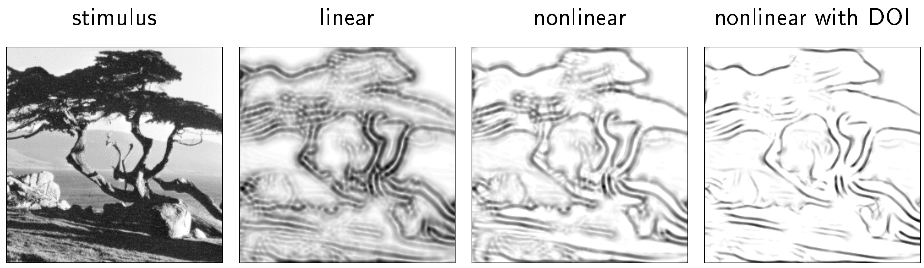

Fig. 4. Natural image of a tree and simulation results.

In the first experiment, we employ a synthetic image of a dark ellipse on a lighter background, corrupted with 50% Gaussian noise. Fig. 3 shows the input stimulus and the simulation results. All models show responses at the edge locations, but only the nonlinear models have a pronounced unimodal response to an edge. Moreover, the results demonstrate that the model with DOI is considerably less sensitive to noise. A further challenge to the model is posed by processing of natural images. We use a tree stimulus shown in Fig. 4. For the

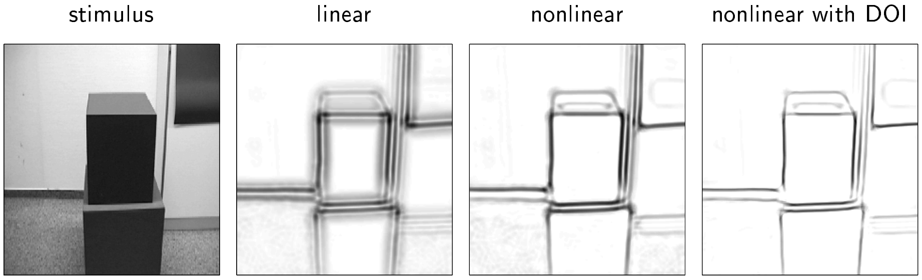

Fig. 5. Image of a laboratory scene and simulation results.

DOI processing, responses to the lawn are largely suppressed, while responses to the contour of the tree and to the shadow are enhanced. We also employ a 3D image of a laboratory scene as input stimulus. Here, the contours of the cube are sharper and the spurious responses at the floor vanish for DOI processing.

5 Simulation of the Hammond & MacKay Study

Hammond and MacKay investigated the response of simple cells in cat to optimally oriented bars (Hammond & MacKay, 1983). Three types of bars where employed: dark bars, dark bars with light segments added in the middle (DLD-bars) and dark bars with light segments added at both ends (LDL-bars). A main result of their work is shown in Fig. 6. The dashed line marks the 'length summation curve' which shows linear response properties up to saturation. When light segments are added to the dark bar (DLD and LDL), the average response decrement is much larger than predicted from linear contrast summation. Linear summation would suggests that the slopes of the curves of length summation and of the combined stimuli are the same.

Our model predicts that simple cell responses as observed by Hammond and MacKay can be generated based on the proposed DOI scheme. Results are shown in Fig. 6 (right). Same model parameters as for the processing of 2D stimuli are employed. The slopes of the curves for both DLD and LDL stimuli decline in a much steeper fashion than for the length summation curve, as reported by Hammond and MacKay. In summary, good qualitative fit with the physiological data is obtained.

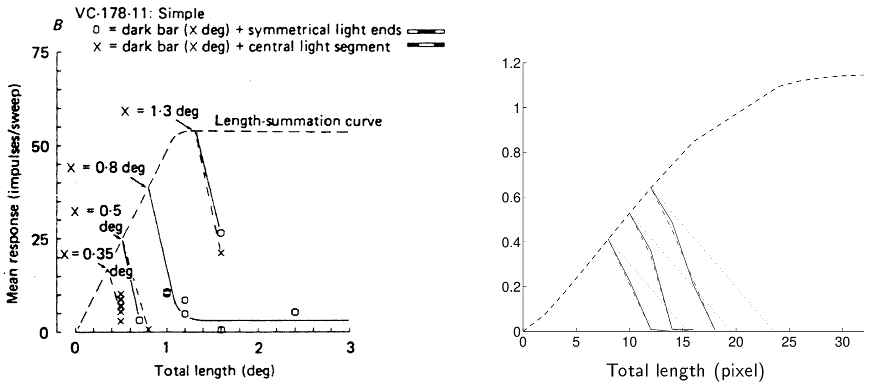

Fig. 6. Hammond and MacKay study (left) and simulation (right). Curves show length summation (dashed), responses to LDL and DLD bars (solid and dash-dotted, resp.) and predictions by contrast summation (dotted).

6 Conclusion

In this work, we propose a scheme of dominating opponent inhibition, extending the functionality of a previously suggested version of a simple cell model. We demonstrate that the extended model is capable of reproducing physiological data on luminance gradient reversal. With identical parameters, we probe the model with noisy 2D stimuli. The results show that sharpness of response and robustness to noise can be increased compared to the previous model.

References

Ferster, D. (1989). The synaptic inputs to simple cells in the cat visual cortex. In D. Lam & C. Gilbert (Eds.), *Neural mechanisms of visual perception* (pp. 63–85). The Woodlands, Texas: Portfolio Publ. Co.

Hammond, P., & MacKay, D. (1983). Influence of luminance gradient reversal on simple cells in feline striate cortex. *J. Physiol.*, *337*, 69–87.

Heggelund, P. (1986). Quantitative studies of enhancement and suppression zones in the receptive field of simple cells in cat striate cortex. *J. Physiol.*, *373*, 293–310.

Hubel, D. H., & Wiesel, T. N. (1962). Receptive fields, binocular interaction and functional architecture in the cat's visual cortex. *J. Physiol.*, *160*, 106–154.

Neumann, H., Pessoa, L., & Hansen, T. (1999). Interaction of ON and OFF pathways for visual contrast measurement. *Biol. Cybern.* (To appear)

Pessoa, L., Mingolla, E., & Neumann, H. (1995). A contrast- and luminance-driven multiscale network model of brightness perception. *Vis. Res.*, *35*(15), 2201–2223.